JOURNAL OF CATALYSIS 151, 285–291 (1995)

Structure and Activity of Molybdenum Oxide Monoatomic Layer Formed on Tin Oxide

Miki Niwa,*,[1] Mitsuru Sano,† Hidenori Yamada,‡ and Yuichi Murakami‡

*Department of Materials Science, Faculty of Engineering, Tottori University, Koyama-cho, Tottori 680 Japan; and †Department of Natural Informatic Science, School of Informatics and Sciences, and ‡Department of Applied Chemistry, School of Engineering, Nagoya University, Furo-cho, Chikusa-ku, Nagoya 464-01 Japan

Received March 4, 1994; revised September 27, 1994

The structure and reducibility of molybdenum oxide supported on tin oxide were studied in order to explain the high activity of molybdenum oxide for the methanol oxidation. Higher reducibility was observed for the molybdenum oxide supported on SnO_2 in comparison with the values for that supported on TiO_2, ZrO_2, and Al_2O_3. The Mo–O bond lengths of the determined molybdenum oxide (0.17, 0.22 nm) on SnO_2 were in agreement with those on the (100) face of MoO_3 which was previously reported to be active for the oxidation; in addition, this had the structure of the active polymeric species. The high activity for the methanol oxidation may be caused by the structure and the reducibility of the loaded molybdenum oxide.

INTRODUCTION

Investigation of the activity of supported metal oxide catalyst is important not only for the development of novel active catalyst but also for deeper scientific understanding of the activity. Current interest in this field is focused on the preparation of thin oxide layer or highly dispersed metal oxide and on identification of its characterization and function. The formation of fine structure could be anticipated, so various methods including spectroscopy and chemical methods are available for the study (1–3).

Our previous investigation revealed that molybdenum oxide was readily spread in less than 7 Mo nm^{-2} and that a monoatomic layer covered the surface of SnO_2 (4), Fe_2O_3 (5), ZrO_2, TiO_2, and Al_2O_3 (6) by ca. 75%, as shown in Fig. 1. The extent of coverage by molybdenum oxide with the surface concentration of Mo, which was determined by a chemical titration method (benzaldehyde–ammonia titration (7)), did not depend upon the kind of supports. The molybdenum oxide monoatomic layer was found to be active for the methanol oxidation and the highest activity was observed on SnO_2. Because we measured the fraction of surface area occupied by loaded molybdenum oxide, the turnover frequency (TOF) for the methanol oxidation was determined based upon the assumption of owned surface area of the molybdenum oxide species. The turnover frequency thus determined depended upon the support and decreased in the order shown above, as shown in Fig. 2. In other words, the TOF of methanol oxidation depended upon the support, although no difference in spreading of molybdenum oxide was observable. The molybdenum oxide monoatomic layer should be in contact with the supports and will be strongly influenced by the structure or chemical property of the basal plane. A subtle difference in structure or different effect induced by the support metal oxide is suspected. By means of laser raman and/or IR spectroscopies, however, we observed the 950 cm^{-1} band which was ascribable to the surface molybdate, but could not find any difference in structures on these supports (4–6).

Tin oxide has a relatively high surface area and amphoteric property, like TiO_2 and ZrO_2, and it is available for the support of metal oxide. Tin oxide as catalyst (8–10), adsorbent (11), and semiconductor gas sensor (12) has been investigated. However, it is not usually used for the support of metal oxide, and there are only a few reports about tin oxide support (13). Thereby, the purpose of this investigation is to determine the structure and reducibility of molybdenum oxide on SnO_2 by X-ray absorption fine structure (XAFS) and Temperature programmed desorption (TPR), respectively, and to correlate them to the catalytic activity. The findings will be compared with the values on other supports. In the study of XAFS, the molybdenum oxide loaded on Al_2O_3 will be used for the comparison because of the low activity.

EXPERIMENTAL METHODS

Catalysts and Oxides

Five kinds of oxides were used as supports for the molybdenum oxide, as shown in Table 1. Tin oxide was prepared from a $SnCl_2$ solution. To the solution, NH_4OH

[1] To whom correspondence should be addressed.

0021-9517/95 $6.00

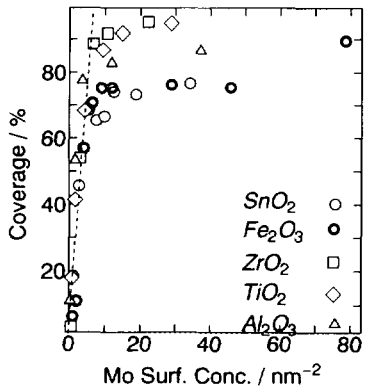

FIG. 1. Spreading of molybdenum oxide on supports; dotted line shows the theoretical relationship between coverage and surface concentration of molybdenum, the molybdenum monoatomic oxide layer being formed.

was added to precipitate the hydroxide, which was then washed until chlorine ion was removed. The hydroxide gel thus obtained was dried and calcined at 773 K for 2 h. Iron oxide and zirconium oxide were prepared by this method from source compounds as mentioned in Table 1. Supported catalysts were prepared by the impregnation method. Supports were added to ammonium heptamolybdate solution, and the pH of the solution was adjusted to 10 by using NH_4OH, since it affected the equilibrium between molybdenum cations in the solution. After excess water was evaporated on a hot plate at 383 K, the precipitate was dried at 393 K for 12 h, followed by calcination at 773 K in a stream of oxygen for 3 h.

Temperature Programmed Reduction

Temperature programmed reduction experiments were carried out using H_2 (6.15%)/Ar mixture as carrier gas. After the catalyst was fully oxidized by oxygen at 773 K, it was reduced by elevating the temperature from 298 to 773 K at a rate of 10 K min^{-1}; consumption of hydrogen was measured by a thermal conductivity detector.

XAFS Measurements

XAFS of molybdenum oxide on supports were measured at BL 10B of Photon Factory at National Laboratory for High-Energy Physics (2.5 GeV) with a storage ring current of ca. 220 mA. The X-rays were monochromatized with Si(311) crystals, and the absorption spectra were obtained using ion chambers from the transmission mode. The sample was compressed into a disk 10 mm in diameter; the standard samples ($Al_2(MoO_4)_3$ and MoO_3) were diluted with alumina and used for the measurements. The photon energy was scanned from 19.65 to 21.00 KeV to detect Mo K-edge spectra.

TABLE 1

Supports Used in This Investigation

Support	Surface area (m^2g^{-1})	Source
SnO_2	24.7	$SnCl_2\,2H_2O$
Fe_2O_3	19.1	$Fe(NO_3)_2$
ZrO_2	66	$ZrOCl_2$
TiO_2	48	Nippon Aerosil, P-25
Al_2O_3	165	JRC-ALO4 (reference catalyst of Catalysis Society of Japan)

The XAFS spectra have been analyzed by following standard procedures. The absorption background before the edge was curve fitted by a modified Victoreen equation, $a\lambda^3 + b\lambda^4 + c$, where λ is the wavelength, and a, b, and c are variable parameters. The absorption spectrum was obtained by subtracting the calculated fitting curve from the measured spectrum, and the resulting spectrum $\mu(k)$ was fitted with a smoothing curve function $\mu_0(k)$ by means of a cubic spline routine. In this procedure, the absorption spectrum above the edge is divided into three regions, each of which is fitted with a third-order polynomial. The individual polynomials are constrained to meet each other with equal slopes at the spline points and combined to form an overall curve for $\mu(k)$. Then, the XAFS, $\chi(k)$, is obtained by $\chi(k) = [\mu(k) - \mu_0(k)]/\mu_0(k)$. The photoelectron wave vector is given by $k = [(E - E_0)2m/\hbar^2]^{1/2}$, where E is the photon energy and E_0 is the reference energy, defined as the energy providing the half of maximum absorption. The Fourier transform was made in the range of 4.0 to 14.0 Å^{-1} of k.

Parameters of the XAFS were determined by a curve-fitting method. The individual peaks of a XAFS Fourier-transformed function, $k^3\chi(k)$, were isolated by using a

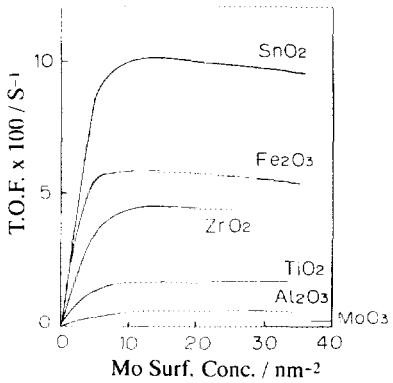

FIG. 2. Turnover frequency of methanol oxidation against the surface concentration of molybdenum on various supports; MoO_3 shows the value on unsupported MoO_3.

proper window function and then Fourier-backtransformed into the momentum space. The resulting filtered signal was fitted with the semi-empirical formula (14)

$$k^3\chi(k) = \Sigma c_0 N R^{-2} \exp(-c_1 k^2) k^{-c2} \sin[a_0 + (a_1 + 2R)k + a_2 k^2],$$

where N and R are the coordination number and the interatomic distance, respectively; c_0, c_1, and c_2 are the parameters for the amplitude functions; and a_0, a_1, and a_2 are the phase shift parameters. Parameters a_0–a_2 and c_0–c_2 of Mo–O were determined experimentally from the structure of standard compounds.

RESULTS

Temperature Programmed Reduction

Reducibility of supported molybdenum oxide was measured by TPR using a hydrogen–argon mixture as carrier gas. Figure 3 shows the TPR on the catalysts where the monoatomic layer of molybdenum oxide covers the surface at ca. 4–7 Mo nm^{-2} of the surface concentration. In this figure, the ordinate is normalized by the number of exposed molybdenum atom which was measured in previous research (4–6). Unsupported molybdenum oxide was not greatly reduced in the present conditions. However, molybdenum oxide supported on Al_2O_3, TiO_2, and ZrO_2 was reduced readily above 500 K. Since little degree of reduction was observed on these supports, hydrogen was consumed to reduce the loaded molybdenum oxide. On the other hand, SnO_2 and Fe_2O_3 were reduced without loading of MoO_3. The loading of molybdenum oxide on SnO_2 enhanced the reduction and gave double peaks of reduction at ca. 590 and 730 K. The intensity on SnO_2 therefore shows the difference between consumed amounts of hydrogen for the reduction of MoO_3/SnO_2 and SnO_2. However, the loading of MoO_3 on Fe_2O_3 suppressed the reduction and shifted the peak maximum temperature from 690 to 720 K. The intensity on Fe_2O_3 in Fig. 3 therefore shows the actual TPR profile on the MoO_3/Fe_2O_3.

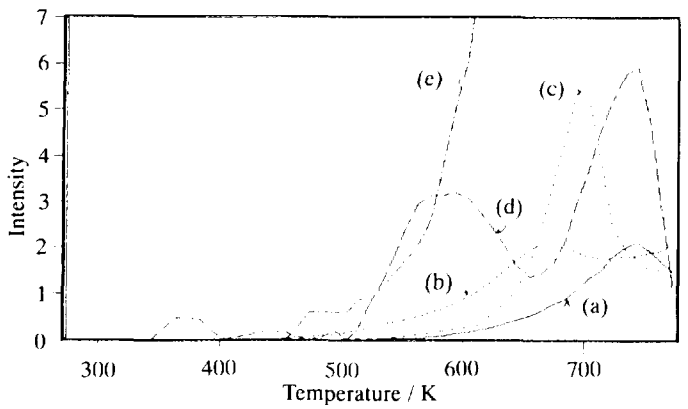

FIG. 3. TPR of molybdenum oxide on supports: (a) 14 wt% (3.7 Mo nm^{-2})MoO_3/Al_2O_3; (b) 5 wt% (4.4 Mo nm^{-2})MoO_3/TiO_2; (c) 10 wt% (6.7 Mo nm^{-2})MoO_3/ZrO_2; (d) 4 wt% (5.5 Mo nm^{-2})MoO_3/SnO_2; (e) 3 wt% (6.5 Mo nm^{-2})MoO_3/Fe_2O_3.

From the comparison of these TPR profiles, it was found that the rate of reduction of the molybdenum oxide monoatomic layer catalyst was rapid on Fe_2O_3 and SnO_2, but it decreased on TiO_2, ZrO_2, and Al_2O_3 in this sequence. The sequence of support for the reducibility of loaded MoO_3 was thereby similar to that of catalytic activity shown above.

The amount of hydrogen consumed could be calculated by the integration of TPR peaks. On SnO_2, however, it was calculated from the TPR intensity only below 663 K, because double peaks were observed, and another peak of reduction at higher temperature seemed to be caused by the reduction of SnO_2 itself. The amount of hydrogen for the reduction of MoO_3 on Fe_2O_3 was not able to be calculated because of the complex behavior. Thus calculated hydrogen monoatom amount divided by exposed molybdenum atom amount was 0.89 (on Al_2O_3), 1.17 (on TiO_2), 1.38 (on ZrO_2), and 1.05 (on SnO_2). Therefore, the ratio of H/Mo was close to 1 on the catalysts except for MoO_3/Fe_2O_3. An exceptionally high value was expected on Fe_2O_3, where bulk oxygens of iron oxide could participate in the reduction through the reduced molybdenum oxide.

XAFS Measurements

Figure 4 shows the Fourier transforms of XAFS spectra of molybdenum on SnO_2 and Al_2O_3 and of reference compounds. We observed peaks at 0.17–0.23 and 0.33–0.41 nm bond length, and identified them as Mo–O and Mo–Mo bonds, respectively. First, the filtered spectrum of the crystalline $Al_2(MoO_4)_3$ with the parameters (r_{Mo-O} = 0.1761 nm and N = 4 (15)) was analyzed in order to determine six parameters (a_0–a_2 and c_0–c_2) by the least-squares fitting method. The XAFS of MoO_3 was then analyzed on the basis of the determined parameters; thus fitted coordination numbers (1.6, 1.6, and 0.94 for bond length 0.170, 0.195, and 0.229 nm, respectively) were, however, smaller than 2, the value for the crystal structure. Because there were approximately three kinds of the bond lengths of Mo–O in MoO_3, three kinds of parameters c_{11}–c_{13} which corresponded to Debye–Waller factors were then determined to fit the coordination number 2, other parameters being unaltered. These eight kinds of parameters were used to determine the bond length and coordination number of supported molybdenum.

The Mo–O bonds were analyzed on the basis of these

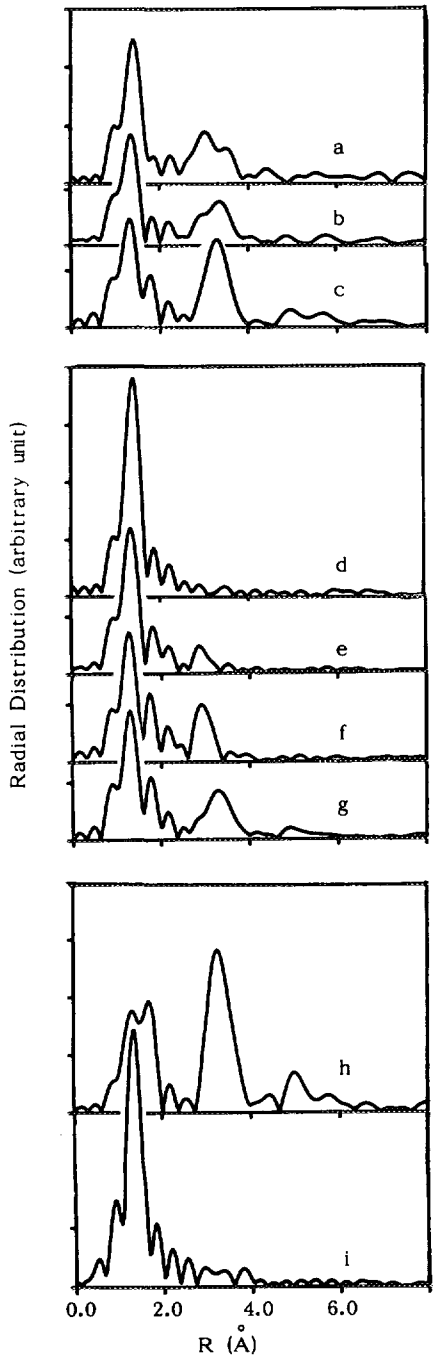

FIG. 4. Fourier transform of the XAFS spectra of (a) 2, (b) 5, and (c) 10 wt% MoO_3 on SnO_2 and of (d) 1.4, (e) 6.9, and (f) 14, and (g) 32 wt% MoO_3 on Al_2O_3 with those of unsupported (h) MoO_3 and (i) $Al_2(MoO_4)_3$.

parameters, and the determined values are shown in Table 2. Figure 5 shows the comparison between the experimental data and the back-Fourier transformed spectrum. The *R*-factors to show the inconsistency between them are shown in Table 2. On the other hand, it was difficult to quantitatively analyze the Mo–Mo bond explicitly because of the large deviation between observed and simulated spectra. However, the Mo–Mo bonds were observed, and the intensity increased with increasing the concentration.

As expected from previous investigations, the bond lengths and coordination numbers of Mo–O of the samples with the large surface concentration (10 wt% on SnO_2 and 32 wt% on Al_2O_3) were almost the same as those of unsupported MoO_3. This is because the concentration of loaded molybdenum oxide was more than needed to cover the surface as the monoatomic oxide layer, and freely isolated MoO_3 was formed (4, 6).

On the other hand, bond lengths and coordination numbers of Mo–O in ≤ 7 Mo nm^{-2} on SnO_2 where the monoatomic oxide layer was identified were different from on the samples with excess MoO_3. The Mo–O bond of bond length of 0.196 nm was missing on 5 wt% (7.7 Mo

TABLE 2

Parameters of Mo–O Measured by XAFS and Turnover Frequency for Methanol Oxidation

Amount loaded surf. conc.	Mo–O bond length (nm)	C.N.[a]	*R*-factor[b] (%)	Turnover Frequency[c] ($10^{-2}s^{-1}$)
On SnO_2				
2 wt%	0.175	2.2	23	4.02
2.8 nm^{-2}	0.217	2.1		
5 wt%	0.172	1.8	18	10.8
7.7 nm^{-2}	0.225	0.7		
10 wt%	0.171	1.9	27	9.99
12.5 nm^{-2}	0.196	0.6		
	0.227	1.3		
On Al_2O_3				
1.4 wt%	0.177	3.8	14	Nil
0.4 nm^{-2}	0.200	0.5		
6.9 wt%	0.175	2.5	21	0.09
1.8 nm^{-2}	0.195	0.4		
	0.233	1.3		
14 wt%	0.172	2.3	25	0.62
3.7 nm^{-2}	0.193	0.9		
	0.230	1.5		
32 wt%	0.173	2.3	27	0.85
11.9 nm^{-2}	0.196	0.8		
	0.231	1.5		
MoO_3	0.170	2		0.24
	0.195	2		
	0.229	2		
$Al_2(MoO_4)_3$	0.176	4		Not measured

[a] Coordination number.

[b] *R*-factor = $\Sigma| |I_0| - |I_{calc}| |/\Sigma|I_0| \times 100$. I_0, Fourier filtered data; I_{calc}, curve fitting data.

[c] Turnover frequency is for the methanol oxidation at 498 K. The occupied surface area of molybdenum species was assumed to be 0.147 nm^2.

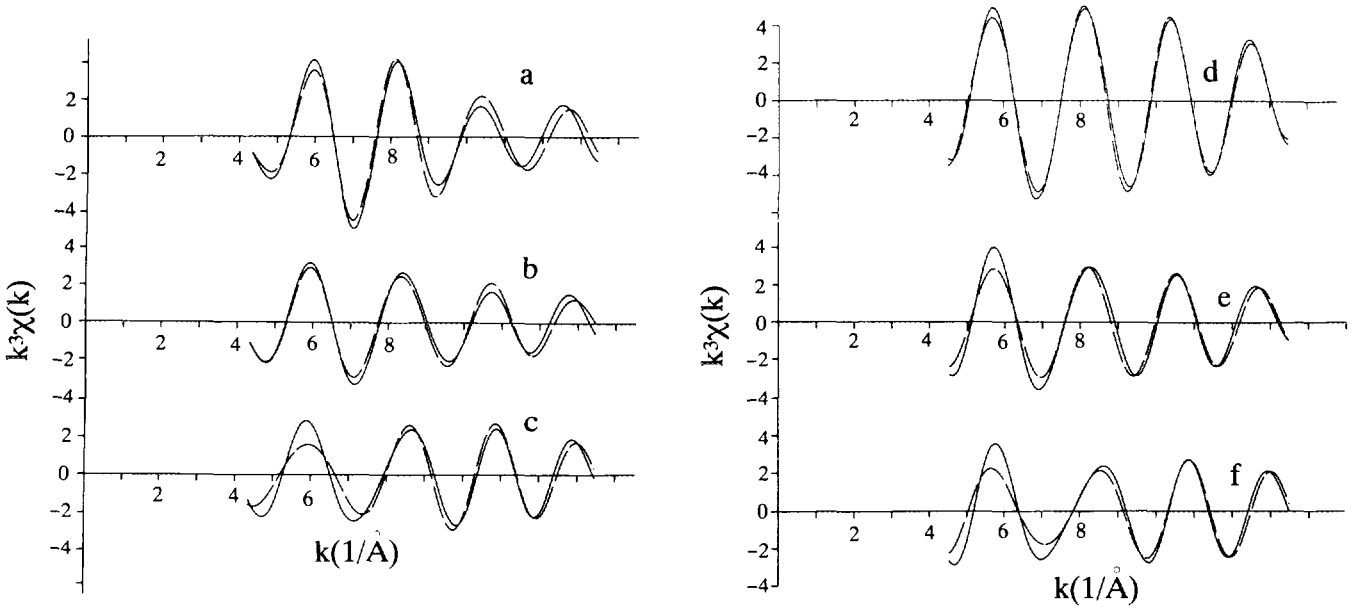

FIG. 5. Fourier filtered XAFS functions (solid line) and their curve fittings (dashed line) for Mo–O on (a) 2, (b) 5, and (c) 10 wt% MoO_3 on SnO_2 and on (d) 1.4, (e) 6.9, and (f) 14 wt% MoO_3 on Al_2O_3.

nm^{-2}) and 2 wt% (2.8 Mo nm^{-2}) loadings on SnO_2. The Mo–Mo bonds were observed in these concentrations, where the intensity decreased with decreasing Mo concentration. The polymeric molybdenum oxide species with two Mo–O bonds was therefore observed on SnO_2, where the extent of polymerization depended upon the surface concentration.

On the other hand, three Mo–O bonds were observed on Al_2O_3 with 14 wt% (3.7 Mo nm^{-2}) and 6.9 wt% (1.8 Mo nm^{-2}) MoO_3. There were Mo–Mo bonds on these samples like on SnO_2. On the 1.4 wt% (0.4 Mo nm^{-2}) loading, a sharp Mo–O peak with coordination number of 3.8 was observed at 0.18 nm. Because this was in agreement with the XAFS on the spinel compound $Al_2(MoO_4)_3$, the MoO_4 species with the tetrahedral configuration was identified on the 1.4 wt% MoO_3/Al_2O_3. The formation of the tetrahedral MoO_4 in low concentrations of molybdenum has been reported from the spectroscopic investigations (16–19). Therefore, the polymeric molybdenum oxide species with three Mo–O bonds was formed on the Al_2O_3 except in the extremely low concentration. Discrimination between tetrahedral and octahedral configurations of molybdenum oxides on Al_2O_3 by XAFS was reported recently, and the dependence on the concentration of loaded MoO_3 was similar to that found in the present investigation (20).

DISCUSSION

It was reported by Kihlborg that the structure of molybdenum trioxide consists of tetrahedral MoO_4 chains, and the buildup of the chains makes the sheet of molybdenum oxide (21). The Mo–O bond lengths of the unit MoO_4 are 0.167, 0.173, and 0.195 nm, and the two neighboring oxygens are at distances of 0.225 and 0.233 nm, as shown in Fig. 6. Because we detected only three Mo–O bonds on unsupported MoO_3 by XAFS measurements, the bond length was determined with an accuracy of 0.01 nm. The three Mo–O bonds observed on Al_2O_3, therefore, can be regarded as all the bonds in the lattice of MoO_3. The molybdenum oxide supported on Al_2O_3 has the structure of the fundamental unit of MoO_3. On the other hand, the molybdenum oxide on SnO_2 lost the Mo–O bond with 0.195 nm of the bond length. In other words, one can conclude, for the molybdenum oxide on SnO_2, that the oxygens in the direction of the c-axis of the MoO_3

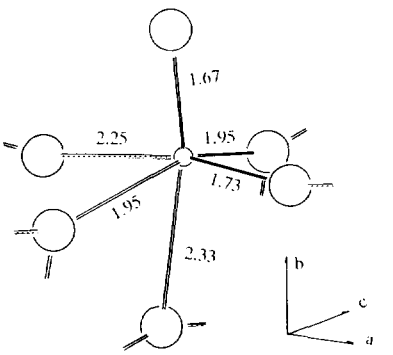

FIG. 6. The coordination of oxygen atoms (large circles) around the molybdenum atom (small circles) in MoO_3 (21).

crystal are lost. Because the MoO_3 on SnO_2 is the most active among the catalysts used in our investigation, the high activity may be caused by the structure.

Volta *et al.*, Tatibouet *et al.*, and Ziolkowski have previously reported that the (100) face of MoO_3 supported on carbon is active for the partial oxidation of alcohol and olefins (22–24); recently, this conclusion was confirmed using unsupported (100)-oriented MoO_3 (25). The bond lengths of Mo–O exposed on the (100) face are 0.173 and 0.225 nm and in good agreement with those of molybdenum oxide on SnO_2. Iwasawa prepared the tailor-made catalyst from a dinuclear molybdenum compound on SiO_2 and determined the structure by means of XAFS at the same station as used in this investigation (26, 27); the prepared dimeric species, which was more active than the mononuclear species, changed the structure during the reaction; however, the oxidized one had the Mo–O bonds of 0.170 and 0.210 nm of the bond length. The chemical bonds of Mo–O, therefore, are similar to those observed on SnO_2. Consequently, these studies consistently showed that the structure of the active molybdenum oxide lost the Mo–O bond of 0.195 nm of the length. It was thereby found that the active molybdenum oxide with the detected chemical bonds of Mo–O was selectively formed on SnO_2 by the usual impregnation method.

On both supports, the neighboring molybdenum can be observed; therefore, the molybdenum species is polymerized (or dimerized) on supports, and the TOF increases with the extent of polymerization. The formation of polymeric molybdenum species, the extent of which depends on the concentration, has been confirmed by various methods, e.g., laser raman spectroscopy (1). Increase of TOF with the extent of polymerization agrees with the mechanism of methanol oxidation previously proposed, in which one molybdenum is used for the adsorption of alcohol and another for the abstraction of hydrogen from the adsorbed methoxide (28–30).

On the other hand, we can identify the high reducibility of molybdenum oxide supported on SnO_2. Because the reducibility was measured from the reduction of molybdenum oxide by hydrogen, it gave us information which was not related to the thermodynamical energy parameter but to the reactivity of molybdenum oxide with hydrogen. In other words, the TPR experiment showed us only the reducibility parameter caused by the most simple reducing molecule. However, the data should be free from the mechanism of the methanol oxidation. It could be therefore concluded from the TPR measurements that molybdenum oxides on SnO_2 and Fe_2O_3 have a weaker bond of Mo–O than on TiO_2, ZrO_2, and Al_2O_3. The strength of the molybdenum–oxygen bond may be influenced by the metal–oxygen bond of supports, because the former metal oxides are more easily reduced than the latter, as confirmed also in this investigation. Therefore, exchange of oxygens between loaded molybdenum oxide and support metal oxide or rapid oxygen supplement to the reduced site from the support is suggested, as has been already claimed by Moro-oka *et al.* in the study of Mo–Bi multicomponent metal oxide catalysts (31). Diffusion of oxygen not only in the lattice of tin oxide but also in the boundary between SnO_2 and MoO_3 could be postulated. However, the TPR did not suggest any deep reduction of support metal oxide, because the stoichiometry of consumed mono-hydrogen atom to reduced molybdenum atom was close to 1, except on Fe_2O_3. The reducibility observed on the molybdenum oxide monoatomic layer may be correlated with the structure, because it could be regarded as a distorted form of molybdenum oxide species and would be identified as a readily reducible species because of the low coordination number.

Various parameters or properties of metal oxides have been proposed to explain not only the behavior of supported metal oxide but also the formation of surface species. Solid acid–basicity (3), electronegativity of cations (32), net pH at the point of zero charge (1, 33), and simply interaction (34) could explain some phenomena of supported metal oxides (e.g., reducibility, spreading, and monomeric and polymeric anion formation). However, these are limited to the overall view of metal oxides supported on broad kinds of metal oxide from acidic SiO_2 to basic MgO. It is actually difficult to understand the behavior of metal oxide on such supports as SnO_2, ZrO_2, TiO_2, and Al_2O_3 on the basis of acidity and basicity parameter. Reducibility parameter might explain the high activity of MoO_3 on Fe_2O_3 and SnO_2; however, it is also difficult to correlate it to the highest activity of MoO_3 on SnO_2. These parameters could explain the whole view of the loaded catalyst, but these could not be applied to the specific activity. Another concept, for example, of both basicity and reducibility may explain the formation of the active molybdenum oxide species and its reducibility. It is now difficult to draw a simple conclusion about the activity of loaded metal oxide based on the property of support.

Solid acidity created in the mixture of SnO_2 and MoO_3 is well known and the activity of oxidation of propylene and methanol was reported to be correlated with the acidity (8, 10). However, the molybdenum oxide monoatomic layer on tin oxide did not have any acidity, as was found from the temperature programmed desorption of ammonia (4). The solid acidity was observed only on the catalyst with excess loading of MoO_3. One can conclude from the present investigation that the oxidation of methanol does not require solid acidity.

CONCLUSION

We studied the high activity of molybdenum oxide on SnO_2 for the methanol oxidation from viewpoints of structure and reducibility. Molybdenum oxide on tin ox-

ide has the structure consisting of two kinds of Mo–O chemical bonds without one fundamental Mo–O bond. It is more readily reduced by hydrogen in compared with MoO_3 unsupported or loaded on other supports. The high activity may be caused by these properties.

REFERENCES

1. Kim, D. S., Segawa, K., Soeya, T., and I. E. Wachs, *J. Catal.* **136,** 539 (1992).
2. Louis, C., Tatibouet, J. M., and Che, M., *J. Catal.* **109,** 354 (1988).
3. Desikan, A. N., Huang, L., and Oyama, S. T., *J. Chem. Soc., Faraday Trans.* **88,** 3357 (1993).
4. Niwa, M., Yamada, H., and Murakami, Y., *J. Catal.* **134,** 331 (1992).
5. Yamada, H., Niwa, M., and Murakami, Y., *Appl. Catal.* **96,** 113 (1993).
6. Matsuoka, Y., Niwa, M., and Murakami, Y., *J. Phys. Chem.* **94,** 1477 (1990).
7. Niwa, M., Inagaki, S., and Murakami, Y., *J. Phys. Chem.* **89,** 3869 (1985).
8. Moro-oka, Y., Takita, Y., and Ozaki, A., *J. Catal.* **27,** 177 (1972).
9. Niwa, M., Mizutani, M., Takahashi, M., and Murakami, Y., *J. Catal.* **70,** 14 (1981).
10. Ai, M., *J. Catal.* **77,** 279 (1982).
11. Harrison, P. G., and Guest, A., *J. Chem. Soc., Faraday Trans. 1* **83,** 3383 (1987).
12. Yamazoe, N., Fuchigami, J., and Kishikawa, M., *Surf. Sci.* **86,** 335 (1979).
13. Reddy, B. M., Narsimha, K., Sivraj, C., and Kantarao, P., *Appl. Catal.* **55,** L1 (1989).
14. Cramer, S. P., Hodgson, K. O., Stiefel, E. I., and Newton, N. E., *J. Am. Chem. Soc.* **100,** 2748 (1978).
15. Rapposch, M. H., Anderson, J. B., and Kostiner, E., *Inorg. Chem.* **19,** 3531 (1980).
16. Hardcastle, F. D., and Wachs, I. E., *J. Phys. Chem.* **95,** 5031 (1991).
17. Zingg, D. S., Makovski, L. E., Tischer, R. E., Brown, R. R., and Hercules, D. M., *J. Phys. Chem.* **84,** 2898 (1980).
18. Hall, W. K., *in* "Proceedings, 4th International Conference on the Chemistry and Uses of Molybdenum" (H. F. Barry and P. C. H. Mitchell, Eds.), p. 224. 1982.
19. Knözinger, H., *in* "Proceedings, 9th International Congress on Catalysis, Calgary, 1988" (M. J. Phillips and M. Ternan, Eds.), Vol. V, p. 20. Chem. Institute of Canada, Ottawa, 1988.
20. Shimada, H., Matsubayashi, N., Sato, T., Yoshimura, Y., Nishijima, A., Kosugi, N., and Kuroda, H., *J. Catal.* **138,** 746 (1992).
21. Kihlborg, L., *Ark. Kemi* **21,** 357 (1963).
22. Volta, J. C., Tatibouet, J. M., Phichitkul, and C., Germain, J. E., *in* "Proceedings, 8th International Congress on Catalysis, Berlin, 1984," Vol. 4, p. 451. Dechema, Frankfurt-am-Main, 1984.
23. Tatibouet, J. M., Germain, J. E., and Volta, J. C., *J. Catal.* **82,** 240 (1983).
24. Ziolkowski, J., *J. Catal.* **80,** 263 (1983).
25. Abon, M., Massardier, J., Mignot, B., Volta, J. C., Floquet, N., and Bertrand, O., *J. Catal.* **134,** 542 (1992).
26. Iwasawa, Y., and Tanaka, H., *in* "Proceedings, 8th International Congress on Catalysis, Berlin, 1984," Vol. 4, p. 381. Dechema, Frankfurt-am-Main, 1984.
27. Iwasawa, Y., Asakura, K., Ishii, H., and Kuroda, H., *Z. Phys. Chem., Neue Folge* **144,** 1005 (1985).
28. Yang, T-J., and Lunsford, J. H., *J. Catal.* **103,** 55 (1987).
29. Chung, J. S., Miranda, R., and Bennett, C. O., *J. Catal.* **114,** 398 (1988).
30. Busca, G., *J. Mol. Catal.* **50,** 241 (1989).
31. Moro-oka, Y., Ueda, W., Tanaka, S., and Ikawa, T., *in* "7th International Congress on Catalysis, Tokyo, 1980" (T. Seiyama and K. Tanabe, Eds.), p. 1086. Elsevier, Amsterdam, 1981.
32. Niwa, M., Matsuoka, Y., and Murakami, Y., *J. Phys. Chem.* **91,** 4519 (1987).
33. Deo, G., and Wachs, I. E., *J. Phys. Chem.* **95,** 5889 (1991).
34. Deo, G., and Wachs, I. E., *J. Catal.* **129,** 307 (1991).